The Equilibrium Structures of Monomeric Group 2 and Lanthanide(II) Metallocenes MCp_2 (M = Ca, Sr, Ba, Sm, Eu, Yb) Studied by ab Initio Calculations

Martin Kaupp,[†] Paul v. R. Schleyer,*[,†] Michael Dolg,[‡] and Hermann Stoll[‡]

Contribution from the Institut für Organische Chemie I, Friedrich-Alexander Universität Erlangen-Nürnberg, Henkestrasse 42, 8520 Erlangen, Germany, and Institut für Theoretische Chemie, Universität Stuttgart, Pfaffenwaldring 55, 7000 Stuttgart 80, Germany.
Received September 20, 1991

Abstract: The equilibrium geometries of the metallocenes MCp_2 (M = Ca, Sr, Ba, Sm, Eu, or Yb) have been studied by ab initio pseudopotential calculations at the Hartree–Fock (HF), MP2, and CISD levels. In the HF calculations all molecules are found to favor regular ("linear") sandwich-type equilibrium structures with increasingly shallow potential energy surfaces for the bending motions along the series M = Ca, Yb, Sr, Eu, Sm, and Ba. Large-scale MP2 calculations for $BaCp_2$ yield a (ring centroid)–Ba–(ring centroid) angle of ca. 147°. However, the linearization energy is less than 1.5 kJ/mol. Thus, barocene can be described as a "quasilinear" molecule. The same description seems appropriate for samarocene and europocene. However, $CaCp_2$ and probably $YbCp_2$ are genuinely linear, whereas $SrCp_2$ is intermediate. The low bending potentials of all species studied (even $CaCp_2$) permit large-amplitude bending motions. Hence, our computational results for these floppy organometallics can be reconciled with the experimentally observed, bent, thermal average, gas-phase structures of the permethylated metallocenes MCp^*_2 (M = Ca, Sr, Ba, or Yb; $Cp^* = \eta_5C_5Me_5$). As is indicated by natural population analysis (NPA), the largely π-type covalent contributions to M–Cp bonding are responsible for the considerably smaller preference for bent structures compared with, e.g., the corresponding dihalides (MX_2) or dimethyl compounds (MMe_2).

Introduction

Practically all structurally characterized "true" organometallic compounds (i.e., the metal is bound to carbon) of Ca, Sr, and Ba involve cyclopentadienyl ligands, either substituted or unsubstituted.[1] The same holds true for the divalent lanthanides, i.e., for Sm(II), Eu(II), and Yb(II) organometallics.[2] Recent experiments have shown that the solvent-free permethylated metallocenes MCp^*_2 ($Cp^* = \eta_5$-C_5Me_5) of these six elements exhibit thermal average structures that are bent (i.e., they have Cp^*–M–Cp^* angles different from 180° but maintain a η_5-coordination), both in the gas phase ($CaCp^*_2$, $SrCp^*_2$, $BaCp^*_2$, and $YbCp^*_2$ have been studied)[3] and in the solid state ($CaCp^*_2$,[4] $BaCp^*_2$,[4] $SmCp^*_2$,[5] $EuCp^*_2$,[5] and $YbCp^*_2$[4b] have been examined).

However, neither of these experimental studies was conclusive with respect to the equilibrium structures of the isolated molecules. Given a relatively shallow potential energy surface for the bending motion (as observed for many heavy alkaline earth MX_2 compounds[6-9]), the thermal average structure observed in the gas-phase electron diffraction experiments may well differ significantly from the equilibrium structure.[3,10] It has been estimated that the energy required to bend a linear molecule by ca. 20° has to be below ca. $RT/2$ to allow for the observed thermal average angles around 150°.[3] This "shrinkage effect"[10] due to large-amplitude motions may be ruled out for the low-temperature solid-state structures. However, intermolecular interactions and crystal packing forces may induce bending in a floppy molecule. Indeed, intermolecular interactions in the solid state are present in varying extents for the MCp^*_2 molecules.[4,5]

All-electron Hartree–Fock calculations on calcocene did not indicate any deviations from a linear sandwich structure, but due to the large errors in the Ca–Cp distance, Blom et al. doubted the reliability of their results for the bending potential.[3d] Quasirelativistic Xα-SW calculations on $YbCp_2$ and $EuCp_2$ also did not reveal any basis in the electronic structure for bent equilibrium geometries.[11] Dolg[12a] has performed calculations on $EuCp_2$ and $YbCp_2$, with his recently developed lanthanide pseudopotentials (including the 4f-electrons as part of the core).[12] However, this study was restricted to D_{5d} and D_{5h} symmetries and did not address the question of bending.

The unusual metallocene geometries are suspected[1-5] to be related to the bent structures of some alkaline earth dihalides that have been a puzzle in main group structural chemistry for more than 25 years.[13] The nonlinear geometries are unexpected as they violate the common models used to predict the geometries of main group compounds.[13] Recently, numerous systematic computational investigations of the bending effects for the heavy alkaline earth dihydrides,[6] dihalides,[7,8] and other MX_2 compounds (X = Li, BeH, BH_2, CH_3, NH_2, or OH)[9] of Ca, Sr, and Ba have been reported (cf. ref 14 for some other related recent studies). The results

[†] Institut für Organische Chemie, Universität Erlangen-Nürnberg.
[‡] Institut für Theoretische Chemie, Universität Stuttgart.

(1) For the most recent review on Ca, Sr, and Ba organometallic chemistry, see: Hanusa, T. P. *Polyhedron* **1990**, *9*, 1345. The recently obtained crystal structure of the [CaR_2(1,4-dioxane)], R = $CH(SiMe_3)_2$, forms a notable exception: Cloke, F. G. N.; Hitchcock, P. B.; Lappert, M. F.; Lawless, G. A.; Royo, B. *J. Chem. Soc., Chem. Commun.* **1991**, 724.

(2) For the most recent review on low-valent lanthanide organometallics, see: Evans, W. J. *Polyhedron* **1987**, *6*, 803.

(3) (a) Andersen, R. A.; Boncella, J. M.; Burns, C. J.; Blom, R.; Haaland, A.; Volden, H. V. *J. Organomet. Chem.* **1986**, *312*, C49. (b) Andersen, R. A.; Blom, R.; Boncella, J. M.; Burns, C. J.; Volden, H. V. *Acta Chem. Scand.* **1987**, *A41*, 24. (c) Andersen, R. A.; Blom, R.; Burns, C. J.; Volden, H. V. *J. Chem. Soc., Chem. Commun.* **1987**, 768. (d) Blom, R.; Faegri, K., Jr.; Volden, H. V. *Organometallics* **1990**, *9*, 372.

(4) (a) Williams, R. A.; Hanusa, T. P.; Huffman, J. C. *J. Chem. Soc., Chem. Commun.* **1988**, 1045. (b) Williams, R. A.; Hanusa, T. P.; Huffman, J. C. *Organometallics* **1990**, *9*, 1128.

(5) Evans, W. J.; Hughes, L. A.; Hanusa, T. P. *J. Am. Chem. Soc.* **1984**, *106*, 4270. Evans, W. J.; Hughes, L. A.; Hanusa, T. P.; Doedens, R. J. *Organometallics* **1986**, *5*, 1285.

(6) Kaupp, M.; Schleyer, P. v. R.; Stoll, H.; Preuss, H. *J. Chem. Phys.* **1991**, *94*, 1360.

(7) Seijo, L.; Barandiaran, Z.; Huzinaga, S. *J. Chem. Phys.* **1991**, *94*, 3762.

(8) Kaupp, M.; Schleyer, P. v. R.; Stoll, H.; Preuss, H. *J. Am. Chem. Soc.* **1991**, *113*, 6012.

(9) Kaupp, M.; Schleyer, P. v. R. *J. Am. Chem. Soc.* **1992**, *114*, 491.

(10) For a recent discussion of gas-phase structure determinations, see, e.g.: Hargittai, I., Hargittai, M., Eds.; *Stereochemical Applications of Gas Phase Electron Diffraction*, Verlag Chemie: Weinheim, 1988.

(11) Andersen, A. A.; Boncella, J. M.; Burns, C. J.; Green, J. C.; Hohl, D.; Rösch, N. *J. Chem. Soc., Chem. Commun.* **1986**, 405. Green, J. C.; Hohl, D.; Rösch, N. *Organometallics* **1987**, *6*, 712. Note that earlier semiempirical EHMO calculations predict $SmCp_2$ to slightly prefer a "linear" structure: Ortiz, J. V.; Hoffmann, R. *Inorg. Chem.* **1985**, *24*, 2095.

(12) (a) Dolg, M. Ph.D. Thesis, University of Stuttgart, 1989. (b) Dolg, M.; Stoll, H.; Savin, A.; Preuss, H. *Theor. Chim. Acta* **1989**, *75*, 173. (c) Dolg, M.; Stoll, H. *Theor. Chim. Acta* **1989**, *75*, 369.

(13) Cotton, F. A.; Wilkinson, G. *Advanced Inorganic Chemistry*, 5th ed.; Wiley: New York, 1988.

(14) v. Szentpály, L.; Schwerdtfeger, P. *Chem. Phys. Lett.* **1990**, *170*, 555. Salzner, U.; Schleyer, P. v. R. *Chem. Phys. Lett.* **1990**, *172*, 461. Hassett, D. M.; Marsden, C. J. *J. Chem. Soc., Chem. Commun.* **1990**, 667. Dyke, J. M.; Wright, T. G. *Chem. Phys. Lett.* **1990**, *169*, 138. DeKock, R. L.; Peterson, M. A.; Timmer, L. K.; Baerends, E. J.; Vernooijs, P. *Polyhedron* **1990**, *9*, 1919.

0002-7863/92/1514-8202$03.00/0

Table I. Comparison of Geometry Parameters Calculated for MCp_2 with Experimental Data for MCp^*_2 (M = Ca, Sr, or Ba)[a]

M	d(Å)	M–C(Å)	α(deg)	C–C(Å)	C–H(Å)	φ(deg)
Ca						
HF[b]	2.428	2.714	linear	1.406	1.066	4.0
MP2[c]	2.332	2.621	linear			
$MP2_{large}$[d]	2.321	2.611	linear			
AE[e]	2.400		linear			
GED[f]	2.312 (6)	2.609 (6)	154 (3)	1.427 (3)		
X-ray[g]		2.64 (2)	147.7, 146.3	1.41 (2)		
Sr						
HF[b]	2.623	2.883	linear	1.406	1.067	4.3
MP2[c]	2.533	2.801	linear			
GED[h]	2.469 (6)	2.750 (8)	149 (3)	1.428 (3)		
Ba						
HF[b]	2.842	3.083	linear[i]	1.405	1.067	4.4
MP2[c]	2.758	3.006	linear[i]			
$MP2_{large}$[d]	2.725	2.976	147.2[i]			
GED[h]	2.631 (6)	2.898 (10)	148 (6)	1.429 (4)		
X-ray[g]		2.99 (2)	130.9, 131.0	1.42 (2)		

[a] See Figure 1 for the definition of internal coordinates. [b] HF calculations with basis sets M 6s6p5d; C [4s4p]/(2s2p); H [4s]/(2s). [c] MP2 calculation; one f-function added to metal basis. The M–ring distance was varied independently, starting from the HF optimized structure. [d] Larger basis: M [7s7p5d1f]/(6s5p5d1f); C [4s4p1d]/(2s2p1d); H [4s]/(2s). [e] All-electron Hartree–Fock calculations (see ref 3d). [f] Thermal average gas-phase structure (see refs 3a,b,d). [g] Thermal average values from crystal structure. Angles for two conformers are given (see ref 4). [h] Thermal average gas-phase structure (see refs 3c,d). [i] Quasilinear, see Table V.

clearly delineate three sets of compounds: molecules with genuinely bent structures (many BaX_2 and some SrX_2 derivatives), those which are definitely linear (all BeX_2 and MgX_2 compounds, some CaX_2 molecules, and $SrLi_2$), and molecules with quasilinear[7] equilibrium geometries (many CaX_2 and SrX_2 compounds and some BaX_2 compounds). The latter species exhibit almost no energy change (<1–2 kJ/mol) when the angles are decreased by ca. 20° from linearity. In these cases no well-defined equilibrium angle can be assigned. The complete set of the Eu and Yb dihalides also has been studied; the structural trends are similar to those of the group 2 dihalides.[12a,15a] Calculations on Sm dihalides indicate these to correspond closely with the Eu species.[15b]

The availability of a consistent set of computational data for a reasonably large number of molecules allows the factors that control the angles and the bending potentials for these species to be delineated.[6-9] Bent geometries are favored by the following: (a) small covalent bonding contributions involving metal d-orbitals that are σ-symmetrical with respect to the two individual M–X bonds (d_{yz} for the molecule placed in the *yz*-plane) and (b) polarization of the metal subvalence shell by the field of the substituents. Factor a corresponds to the covalent "d-hybridization" model employed by Hayes,[16] whereas factor b is equivalent to the "reverse polarization" argument of the polarized ion model.[17] While the merits of the two models have been debated, our pseudopotential results for the alkaline earth dihydrides[6] and dihalides[8] indicate both factors to be important. In their model potential study of the dihalides[7] Seijo et al. also found that contributions from the $(n-1)$-d-orbitals *and* the nonfrozen-core behavior of the metal $(n-1)$-p-orbitals have to be taken into account for quantitatively correct results. Of course, the major factor opposing a bent geometry for these (mostly very ionic) molecules is the mutual repulsion of the substituents.[8] Additionally, in MX_2 compounds with groups bearing extra lone pairs (e.g., X = NH_2, OH, or F), small π-bonding contributions also favor linear geometries. This accounts for our unexpected prediction that the dimethyl compounds of Sr and Ba are more strongly bent than the corresponding difluorides.[9]

Due to a combination of these factors the preference for bent equilibrium structures increases in going from Ca to Ba[6-10] and decreases in the order Ba(II)[7,8] > Sm(II)[12a,15b] ≈ Eu(II)[12a,15a] > Yb(II).[12a,15a] Hence, any deviation from linearity for the metallocenes should be largest with M = Ba (except, maybe, for the hypothetical radocene). In view of the good performance of the quasirelativistic 10-valence-electron pseudopotential approach with compounds of Ca, Sr, and Ba,[6,8,9] and Ln(II)[12,15] we have carried out full geometry optimizations (within C_s symmetry) at the Hartree–Fock level of theory and further calculations, including electron correlation corrections at the MP2 level, for MCp_2 (M = Ca, Sr, Ba, Sm, Eu, or Yb). For $EuCp_2$ and $YbCp_2$ some CISD calculations are presented. The MCp_2 electronic structures are compared to those of other MX_2 species to rationalize the observed structural trends.

Computational Details

The quasirelativistic 10-valence-electron pseudopotentials for Ca, Sr, and Ba and the corresponding 6s6p5d basis sets have been published earlier.[6] For MP2 calculations, one set of metal f-functions was added.[6] A pseudopotential to replace the He-core,[18] and a corresponding [4s4p]/(2s2p) valence basis set[19] have been used for carbon. The [4s]/(2s) basis set of Dunning and Hay[20] was employed for hydrogen. For calcocene and barocene, some MP2 calculations with [7s7p5d1f]/(6s5p5d1f) metal basis sets[21] and a set of d-functions added on carbon ($\alpha = 0.6$)[22] have been performed (designated as $MP2_{large}$).

Quasirelativistic 10-valence-electron pseudopotentials (with fixed $[Kr]4d^{10}4f^6$, $[Kr]4d^{10}4f^7$, and $[Kr]4d^{10}4f^{14}$ core occupations for Sm, Eu, and Yb, respectively) and the corresponding [7s6p5d]/(5s4p3d) valence basis sets have been employed for Ln(II).[12] In MP2 and CI calculations, one set of f-functions[12] was added. The carbon and hydrogen basis sets were those described above (calculations including a polarization d-function on carbon are designated as $MP2_{large}$).

Staggered conformations of the two Cp rings were assumed;[3] this reduced the symmetry from D_{5d} to C_s when the Cp–M–Cp angles were lower than 180°. The Hartree–Fock geometry optimizations were carried out with the Gaussian 88[23] and partly with the TURBOMOLE[24] programs, using standard gradient techniques. The group 2 and lanthanide(II) metallocenes were fully optimized within C_s symmetry. Semidirect MP2 calculations combined with a direct SCF scheme employed the Gaussian 90[25] and TURBOMOLE[24] codes. These programs allowed

(15) (a) Dolg, M.; Stoll, H.; Preuss, H. *THEOCHEM* **1991**, *235*, 67. (b) Kaupp, M. Unpublished results.
(16) Hayes, E. F. *J. Phys. Chem.* **1966**, *70*, 3740.
(17) Guido, M.; Gigli, G. *J. Chem. Phys.* **1976**, *65*, 1397.
(18) Igel-Mann, G.; Stoll, H.; Preuss, H. *Mol. Phys.* **1988**, *65*, 1321.
(19) (a) Kaupp, M.; Stoll, H.; Preuss, H. *J. Comput. Chem.* **1990**, *11*, 1029. (b) Poppe, J.; Igel-Mann, G.; Savin, A.; Stoll, H. Unpublished results.
(20) Dunning, T. H.; Hay, P. J. In Schaefer III, H. F. (Ed.): *Methods of Electronic Structure Theory*; Plenum Press: New York, 1977; Modern Theoretical Chemistry, Vol. 3, p 1 ff.
(21) Kaupp, M. Unpublished results.
(22) Huzinaga, S., Ed.; *Gaussian Basis Sets for Molecular Calculations*; Elsevier: New York, 1984.
(23) Frisch, M. J.; Head-Gordon, M.; Schlegel, H. B.; Raghavachari, K.; Binkley, J. S.; Gonzalez, C.; DeFrees, D. J.; Fox, D. J.; Whiteside, R. A.; Seeger, R.; Melius, C. F.; Baker, J.; Kahn, L. R.; Stewart, J. J. P.; Fluder, E. M.; Topiol, S.; Pople, J. A. *Gaussian 88*; Gaussian, Inc.: Pittsburgh, PA, 1988.
(24) Program package TURBOMOLE: Ahlrichs, R.; Bär, M.; Häser, H.; Horn, H.; Kölmel, K. *Chem. Phys. Lett.* **1989**, *162*, 165.

Table II. Comparison of Geometry Parameters Calculated for MCp_2 with Experimental Data for MCp^*_2 (M = Sm, Eu, or Yb)[a]

M	d(Å)	M–C(Å)	α(deg)	C–C(Å)	C–H(Å)	φ(deg)
Sm						
HF[b]	2.701	2.953	linear	1.406	1.067	4.5
MP2[c]	2.620	2.880	164.4[d]			
$MP2_{large}$[c,e]	2.593	2.855	169.6[d]			
X-ray[f]		2.79 (1)	140.1	ca. 1.37–1.43		
Eu						
HF[b]	2.677	2.932	linear	1.407	1.075	4.3
MP2[c]	2.597	2.859	175.2[d]			
CISD[g]	2.628 (2.617)					
$CISD_\pi$[g,h]	2.659 (2.660)					
Dolg[i]	2.666 (2.590)	2.922 (2.839)		1.406	1.072	3.5
X-ray[f]		2.79 (1)	140.3	ca. 1.37–1.45		
Yb						
HF[b]	2.566	2.831	linear	1.407	1.074	4.1
MP2[c]	2.474	2.748	linear			
CISD[g]	2.505 (2.493)					
$CISD_\pi$[g,h]	2.540 (2.540)					
Dolg[i]	2.541 (2.456)	2.803 (2.709)		1.408	1.072	3.7
GED[j]	2.326 (5)	2.622 (6)	158 (4)	1.428 (4)		
X-ray[k]		2.665 (3)	ca. 145			

[a] See Figure 1 for the definition of internal coordinates. [b] HF calculations with basis sets M [7s6p5d]/(5s4p3d); C [4s4p]/(2s2p); H [4s]/(2s). [c] MP2 calculation, one f-function added to metal basis. The M-ring distance was varied independently, starting from the HF optimized structure. [d] Quasilinear, see Table V. [e] One set of d-functions (α = 0.6) added on carbon. [f] Thermal average values from crystal structure (see ref 5). [g] Singles + doubles configuration interaction calculations. Results with Davidson's size consistency correction (cf. ref 37) added are given in parentheses. One metal f-function and one carbon d-function added. All 60 electrons correlated. [h] Only the ligand π-system and the Ln 6s orbital (12 electrons) were correlated. [i] Pseudopotential HF calculations by Dolg (ref 12a), same metal basis sets as employed in this study, but all-electron treatment for C using double ζ basis sets with one polarization function on C and H, respectively. MP2 values (with one metal f-function) are given in parentheses. [j] Thermal average gas-phase structure (see refs 3a,b). [k] X-ray structure (cf. ref 4b).

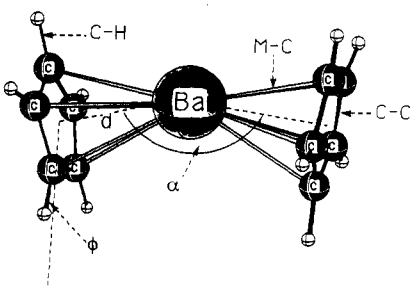

Figure 1. Definition of internal coordinates for MCp_2.

separate optimizations of the metal–(ring centroid) distances and scans of the bending potentials by MP2 single point calculations for all species. The complete MO space available outside the pseudopotential cores was correlated. Additional CISD calculations with the MOLPRO program[26] have been carried out to study correlation effects for the $EuCp_2$ and $YbCp_2$ M–Cp distances (in D_{5d} and D_{5h} symmetries). The largest CI expansions (all 60 electrons correlated) contained ca. 2.85×10^6 configurations. Natural population analyses (NPA) employed Reed's Gaussian 88 adaptation of the NBO program.[27]

Results and Discussion

A. Metal–Ring Distances. As the apparent discrepancy between calculated and experimental (gas-phase) metal–(ring centroid) distances has been interpreted to indicate the general unreliability of the calculated calcocene structures by Blom et al.,[3] we will discuss this problem first, before addressing the question of the Cp–M–Cp angle. (For the definition of the internal coordinates, see Figure 1.) The main geometry parameters for the optimized metallocene structures are summarized in Tables I and II, together with the available gas-phase electron diffraction and solid-state MCp^*_2 structural data (as indicated by the computations of Blom et al.,[3d] the influence of the methyl substitution on the main structural features of the monomers probably is minor).

The metal–(ring centroid) distances *d* calculated at the Hartree–Fock (HF) level of theory overestimate the experimental MCp^*_2 gas-phase values by ca. 12, 15, 21, and 24 pm for M = Ca, Sr, Ba, and Yb, respectively (as the bond lengthening due to intermolecular forces in the solid-state structures is difficult to assess, we will not use these values for comparison). The differences in the M–C distances, which are directly observable in the experiment, are ca. 10, 13, 18, and 21 pm along this series (the experimental average values have been employed, see Tables I and II). The Ca–C distances for calcocene obtained at the SCF level are in reasonable agreement (ca. 3 pm larger) with the previous Hartree–Fock calculations of Blom et al.,[3d] and the values for $YbCp_2$ and $EuCp_2$ are only slightly (1–2 pm) larger than those obtained by Dolg[12a] with polarization functions on carbon and hydrogen. Optimization of the M–Cp distance at the MP2 level (including one f-function on the metal) reduces the M–C separations considerably. However, they are still too large by ca. 5, 11, and 13 pm for M = Sr, Ba, and Yb, respectively. Only the value obtained for $CaCp_2$ is very close (ca. 1 pm) to experiment. The MP2 M–C distances for $EuCp_2$ and $YbCp_2$ are again slightly (2–4 pm) larger than those obtained by Dolg.[12a] The inclusion of d-functions on carbon in our calculations on $EuCp_2$ and $YbCp_2$ shortens the M–C distances by 1.5 pm at the HF level. Interestingly, CISD calculations[26] virtually reproduce the SCF values when only the π-orbitals of the ligands and the lanthanide 6s-orbital are included in the active space (cf. Table II). This agrees with previous results on ferrocene.[28,29] When all electrons are correlated, the CISD and MP2 results are very similar. For $BaCp_2$, $CaCp_2$, and $SmCp_2$ we have performed MP2 calculations including d-functions on carbon (and slightly different Ca and Ba basis sets, see preceding section). These calculations are designated as $MP2_{large}$. At this level the M–C distances for $BaCp_2$ and $SmCp_2$ are reduced further by ca. 3 pm, but for barium the difference compared with the experimental value is still 8 pm. The Ca–C distance in $CaCp_2$ is reduced only very slightly (by ca. 1

(25) Frisch, M. J.; Head-Gordon, M.; Trucks, G. W.; Foresman, J. B.; Schlegel, H. B.; Raghavachari, K.; Robb, M.; Binkley, J. S.; Gonzalez, C.; DeFrees, D. J.; Fox, D. J.; Whiteside, R. A.; Seeger, R.; Melius, C. F.; Baker, J.; Kahn, L. R.; Stewart, J. J. P.; Topiol, S.; Pople, J. A. *Gaussian 90, Revision F*; Gaussian, Inc.: Pittsburgh, PA, 1990.

(26) Program system MOLPRO: Werner, H.-J.; Knowles, P. J. *J. Chem. Phys.* **1988**, *89*, 5803. Knowles, P. J.; Werner, H.-J. *Chem. Phys. Lett.* **1988**, *145*, 514.

(27) (a) Reed, A. E.; Weinstock, R. B.; Weinhold, F. *J. Chem. Phys.* **1985**, *83*, 735. (b) Reed, A. E.; Weinhold, F. *J. Chem. Phys.* **1985**, *83*, 1736. (c) Reed, A. E.; Curtiss, L. A.; Weinhold, F. *Chem. Rev.* **1988**, *88*, 899.

(28) Lüthi, H. P.; Ammeter, J. H.; Almlöf, J.; Faegri, K. *J. Chem. Phys.* **1982**, *77*, 2002. Almlöf, J.; Faegri, K.; Schilling, B. E. R.; Lüthi, H. P. *Chem. Phys. Lett.* **1984**, *106*, 266. Lüthi, H. P.; Siegbahn, P. E. M.; Almlöf, J.; Faegri, K.; Heiberg, A. *Chem. Phys. Lett.* **1984**, *111*, 1.

(29) Park, C.; Almlöf, J. *J. Chem. Phys.* **1991**, *95*, 1829.

Table III. Calculated Energies for the Reaction: $M^{+2} + 2X^- \rightarrow MX_2$ (M = Ca, Sr, Ba, Eu, or Yb; X = F, Cl, Br, I, or Cp)[a]

	X				
M	F	Cl	Br	I	Cp
Ca	−2498	−1842	−1821	−1693	−2050
Sr	−1990	−1709	−1646	−1570	−1911
Ba	−1847	−1581	−1521	−1449	−1781
Eu	−1906	−1677	−1636	−1588	−1885
Yb	−2040	−1752	−1710	−1659	−1966

[a] The energies (in kJ/mol) have been obtained at the Hartree–Fock level for linear MX_2 geometries. Computational details for the dihalides are given in refs 8 and 15a.

pm compared to the MP2 value without d-functions on carbon) and now essentially reproduces the experimental gas-phase value.[3]

We can compare these errors in the metal–ligand distances to those obtained at the Hartree–Fock level with the same metal basis sets in the alkaline earth dihalides.[8] The errors for the metallocenes are about twice as large as those for the diiodes and dichlorides (where relatively accurate recent experimental data are available). The relative reduction of the error at the MP2 level for the metallocenes is in the same range as in corresponding configuration interaction calculations for the dichlorides and diiodides.[8] The high sensitivity of the M–Cp distance to correlation effects might be due to the weakness of the bond. However, the M–(ring centroid) and M–C distances (cf. Tables I and II), the heterolytic dissociation energies (cf. Table III), and the symmetric M–Cp stretch force constants (the values between ca. 2.3 mdyn/Å for $BaCp_2$ and ca. 2.9 mdyn/Å for $CaCp_2$ obtained at the HF level are well in the range of the results for the difluorides and dichlorides)[8] indicate that the ionic M–Cp bond is neither weaker nor longer than the bond in, e.g., the dichlorides.

To obtain accurate metal–ligand distances, strongly correlated wave functions with even larger basis sets and the inclusion of higher excitations probably would be necessary (particularly for the heavier metals Ba, Sm, Eu, and Yb). This is similar to the situation for ferrocene.[28,29] Interestingly, the most recent work on $FeCp_2$[29] indicates that dynamic correlation (including the Fe 3s and 3p orbitals) is essential to reproduce the experimental Fe–Cp distance, in contrast to earlier studies which emphasized the typical transition-metal near-degeneracy correlation effects.[28] A similar sensitivity of the metal–(ring centroid) distances to correlation is observed for the η_5-cyclopentadienides of K, Rb, and Cs and for CpZnMe,[30] while the M–Cp distances in LiCp[31] and $MgCp_2$[32] appear to be influenced only slightly. Further investigations into the origin of these effects are in progress.[30] With respect to section B, it is important to stress that the experimental Ca–Cp distance in calcocene is reproduced excellently by the MP2 calculations, in contrast to the other species studied in this work.

B. Angular Geometry and Potential Energy Surface for the Bending Motions. Full Hartree–Fock optimizations in C_s symmetry yield regular (linear) sandwich-type equilibrium structures with D_{5d} symmetry for all six metallocenes (see Tables I and II). Similarly, optimizations in C_{2v} symmetry for $EuCp_2$ and $YbCp_2$ gave D_{5h} equilibrium structures which are energetically less than 0.1 kJ/mol above the D_{5d} geometries. This is in contrast to the bent arrangements determined experimentally, both in the gas-phase thermal average and in the solid-state structures of MCp^*_2 (cf. Tables I and II). Note that the group 2 metal basis sets employed here are the same used in our study of the alkaline earth dihalides.[8] For example, CaF_2, which has a very shallow bending potential, was found to favor a bent minimum, both at the SCF and at the SDCI levels of theory.[8] A significant underestimation of the bending in the metallocenes due to basis-set deficiencies at the Hartree–Fock level of theory seems unlikely. Correlation

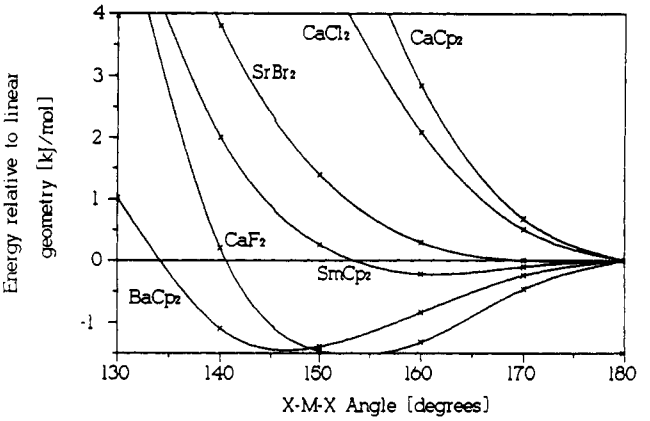

Figure 2. Energy change with X–M–X angle for $CaCp_2$, $BaCp_2$, $SmCp_2$, and various group 2 dihalides (the best MP2 values have been plotted, see Table IV).

Table IV. Calculated Energy Change upon Bending for Various MX_2 Species[a]

	X–M–X angle (deg)			
species	180	170	160	150
MgF_2[b]	0.00	1.49	6.17	14.50
$CaCl_2$[b]	0.00 (0.00)	0.50 (0.50)	2.10 (2.08)	5.08 (4.83)
$SrBr_2$[b]	0.00 (0.00)	0.10 (0.00)	0.65 (0.29)	2.14 (1.39)
CaF_2[b]	0.00 (0.00)	−0.13 (−0.46)	−0.13 (−1.32)	0.19 (−1.46)
$CaCp_2$	0.00 (0.00) (0.00)[d]	0.90 (0.73) (0.67)[d]	3.82 (3.11)[c] (2.84)[d]	9.44 (7.13)[d]
$SrCp_2$	0.00 (0.00)	0.53 (0.47)	2.27 (2.06)	5.66
$BaCp_2$	0.00 (0.00) (0.00)[d]	0.09 (0.08) (−0.24)[d]	0.48 (0.41) (−0.84)[d]	1.55 (−1.39)[d]
$SmCp_2$	0.00 (0.00) (0.00)[d]	0.32 (−0.09) (−0.10)[d]	1.38 (−0.09) (−0.22)[d]	3.62 (0.70) (0.26)[d]
$EuCp_2$	0.00 (0.00)	0.46 (0.00)	1.61 (0.26)	4.11
$YbCp_2$	0.00 (0.00)	0.78 (0.52)	3.14 (2.32)	7.43 (6.02)

[a] In kJ/mol. Hartree–Fock results with MP2 values (one f-function added to the metal basis) in parentheses. Only the X–M–X angle was varied; all other internal coordinates were kept fixed. [b] Computational details for the dihalides (basis sets for Mg, F, Cl, and Br) are given in ref 8. [c] The difference between 160° bent and linear structure obtained by Blom et al. (Hartree–Fock all-electron calculation, see ref 3d) is 3.5 kJ/mol. [d] MP2 calculation with large basis on Ca and Ba, and d-functions on carbon ($MP2_{large}$). The barocene results for smaller angles are: −1.10 kJ/mol (140°), +1.02 kJ/mol (130°).

corrections were found to have only a modest impact on the angles and the characteristics of the bending potentials of the group 2 dihydrides[6] and dihalides.[8]

However, this is only valid if the potential energy surface is not exceedingly flat. The equilibrium structures obtained for quasilinear molecules may be fortuitous. It is important to evaluate the bending potential. Neither a complete surface scan nor a complete harmonic frequency analysis at a reasonable level of ab initio theory is feasible at present for the metallocenes. Therefore we have performed single point calculations with Cp–M–Cp angles fixed at 180°, 170°, 160°, and 150°, starting from the fully optimized (D_{5d}) structures and keeping all other parameters constant (this method has been employed earlier for $CaCp_2$[3d]). For comparison, such calculations have also been carried out for MgF_2, CaF_2, $CaCl_2$, and $SrBr_2$. For the last set of molecules more detailed information on the bending potential (e.g., harmonic vibrational frequencies) is available.[7,8] MgF_2 and $CaCl_2$ have been chosen to represent genuinely linear species,[7,8,10,33] whereas CaF_2 and $SrBr_2$ are classified as quasilinear.[7,8] MgF_2 is more rigid than $CaCl_2$. The energy changes for angles below 180° are displayed in Table IV, while Figure 2 gives graphical representations of the

(30) Lambert, C.; Kaupp, M.; Schleyer, P. v. R.; Stoll, H. To be published.
(31) (a) Jemmis, E. D.; Schleyer, P. v. R. *J. Am. Chem. Soc.* **1982**, *104*, 4781. (b) Waterman, K. C.; Streitweiser, A. C., Jr. *J. Am. Chem. Soc.* **1984**, *106*, 3138. (c) Blom, R.; Faegri, K., Jr.; Midtgaard, T. *J. Am. Chem. Soc.* **1991**, *113*, 3230.
(32) Faegri, K., Jr.; Almlöf, J.; Lüthi, H. P. *J. Organomet. Chem.* **1983**, *249*, 303.
(33) (a) White, D.; Calder, G. V.; Hemple, S.; Mann, D. E. *J. Chem. Phys.* **1973**, *59*, 6645. (b) Vajda, E.; Hargittai, M.; Hargittai, I.; Tremmel, T.; Brunvoll, J. *Inorg. Chem.* **1987**, *26*, 1171. (c) Ramondo, F.; Bencivenni, L.; Nunziante Cesaro, S.; Hilpert, K. *J. Mol. Struct.* **1989**, *192*, 83.

Table V. NPA Metal Charges Q(M) and Metal NAO Valence Populations for the Ca, Sr, and Ba Metallocenes and Dibromides and for the Sm, Eu, and Yb Metallocenes[a]

species	Q(M)	s	p_x	p_y	p_z	d_{xy}	d_{xz}	d_{yz}	$d_{x^2-y^2}$	d_{z^2}
$CaCp_2$	1.847	0.045	0.017	0.017	0.001	0.001	0.034	0.034	0.002	0.004
$CaBr_2$	1.808	0.081	0.008	0.007	0.007	0.000	0.023	0.023	0.000	0.043
$SrCp_2$	1.867	0.032	0.016	0.016	0.001	0.000	0.032	0.032	0.001	0.004
$SrBr_2$	1.848	0.054	0.005	0.005	0.007	0.000	0.023	0.023	0.000	0.040
$BaCp_2$	1.872	0.017	0.013	0.013	0.001	0.000	0.041	0.041	0.001	0.004
$BaBr_2$	1.875	0.024	0.003	0.003	0.001	0.000	0.025	0.025	0.000	0.046
$SmCp_2$	1.899	0.004	0.015	0.015	0.001	0.000	0.036	0.036	0.000	0.004
$EuCp_2$	1.901	0.004	0.015	0.015	0.001	0.000	0.034	0.034	0.000	0.004
$YbCp_2$	1.913	0.005	0.016	0.016	0.001	0.000	0.027	0.027	0.000	0.003

[a] The charges Q(M) do not exactly match $2 - \sum$pop, as some minor contributions from Rydberg NAOs are neglected. All numbers pertain to linear structures (only $BaBr_2$ is found bent at this level of theory). The main molecular axis is the z-axis. The HF wave functions have been analyzed. Note, that the lanthanide metal basis set size is different from that of the group 2 basis sets. For the [5s5p1d]/(3s3p1d) bromine valence basis sets, see ref 8.

best MP2 calculations for CaF_2, $CaCl_2$, $SrBr_2$, $CaCp_2$, $BaCp_2$, and $SmCp_2$.

At the HF level all MCp_2 molecules exhibit a minimum at linear geometries. The MCp_2 HF bending potential becomes increasingly shallow along the series M = Ca, Yb, Sr, Eu, Sm, and Ba, in excellent agreement with the trend of the solid-state Cp–M–Cp angles.[4,5] Due to different basis set requirements, this clear trend does not hold at the MP2 level (without d-functions on carbon). Particularly for $BaCp_2$, the correlation corrections employed appear to be insufficient (see above for the discussion of the M–C distances). Therefore we have studied the bending potentials for the representative systems, $CaCp_2$, $BaCp_2$, and $SmCp_2$, with larger basis sets including d-functions on carbon (designated $MP2_{large}$, see Computational Details). At this level, $BaCp_2$ and $SmCp_2$ exhibit very shallow minima at Cp–M–Cp angles of ca. 147° and ca. 170° (with linearization energies of ca. 1.4 and 0.2 kJ/mol), respectively. Compared with CaF_2 (see Figure 2, Table IV) barocene (and $SmCp_2$ even more so) should probably also be classified as quasilinear. $CaCp_2$, on the other hand, exhibits a relatively shallow (e.g., compared to $MgCp_2$)[3d] but significant potential well at 180° in all calculations. Allowing for relaxation of the other structural parameters (Ca–Cp distance, ring geometry) upon bending might lead to a further slight flattening of the well. However, this would not alter the qualitative conclusion that calcocene is a genuinely linear molecule (note, that the Ca–Cp distance at the MP2 level of theory agrees well with experiment) and comparable in this respect to $CaCl_2$.[7,8,10,33] The bending potentials for all six metallocenes studied are quite shallow. $EuCp_2$ appears to be quasilinear and very similar to $SmCp_2$. $YbCp_2$, on the other hand, is probably linear like $CaCp_2$. $SrCp_2$ is found to be linear at the levels of theory employed. However, the energy difference between structures with Cp–Sr–Cp angles of 180° and 160° might be below 1 kJ/mol in more accurate calculations. This would bring strontocene into the "quasilinear" category. Of course, there are no clearcut thresholds for such classifications.

Thermal average angles of ca. 145–155° in GED experiments have been observed[10,33b,34a,b] for many alkaline earth dihalides with reputedly linear[7,8,10,33a,c,34c] equilibrium geometries. These thermal average structures have been obtained at higher temperatures (above 1000 K). But even for the temperatures pertaining to the MCp^*_2 structure determinations (ca. 430–540 K)[3] the $RT/2$ term corresponds to ca. 2 kJ/mol. The deformation of a linear structure to ca. 160° should require less than $RT/2$ to bring linear equilibrium geometries and the observed bent thermal average structures for the metallocenes into agreement.[3] The energy values in Table IV show this condition to be clearly fulfilled for $SrCp_2$ and the quasilinear species $BaCp_2$, $SmCp_2$, and $EuCp_2$ and approximately fulfilled for linear $CaCp_2$ and $YbCp_2$. The energy needed to bend calcocene to 160° is below 3 kJ/mol at the MP2 level (the previous Hartree–Fock study of calcocene gives a value of ca. 3.5 kJ/mol).[3d] Relaxation of all nuclear coordinates upon bending would certainly, to some extent, reduce these values. Thus, there is no fundamental contradiction between the computed linear equilibrium geometry and the bent gas-phase thermal average structures for $CaCp_2$ and $YbCp_2$.

C. Other Geometrical Features. The calculated C–C distances in MCp_2 (M = Ca, Sr, Ba, or Yb) are ca. 2.5 pm shorter than the experimental values in MCp^*_2 (cf. Tables I and II), which is approximately the expected magnitude of underestimation at the Hartree–Fock/double-ζ basis set level.[31,32] The hydrogen atoms are slightly (ca. 4°) bent away from the metal. This is in agreement with previous computational studies on ionic metallocenes.[31,32] The bending effect may be rationalized either by simple electrostatic considerations or within an MO framework.[31a,b] The value of the out-of-plane angle φ would probably slightly decrease upon addition of d-functions on carbon[31b] (compare Table II for the angles given by Dolg[12a]).

D. Electronic Structure and Bending Potential. Apparently, the preferences for bent structures are significantly smaller for the Ca, Sr, and Ba metallocenes than for the corresponding dihalides[7,8] or for the dimethyl compounds.[9] $Ba(CH_3)_2$, $Sr(CH_3)_2$, BaF_2, and SrF_2, for example, are genuinely bent molecules, whereas $CaMe_2$ and CaF_2 are both quasilinear.[7-9] Barocene is quasilinear, and calcocene is linear. Similar comparisons can be made for $SmCp_2$, $EuCp_2$, and $YbCp_2$ and the corresponding dihalides.[15] This reduced preference of the metallocenes for bent structures can be attributed to differences in the small covalent bonding contributions. Table V compares the natural atomic orbital (NAO)[27] populations of the Ca, Sr, and Ba metallocenes with those of the corresponding dibromides. The populations for $SmCp_2$, $EuCp_2$, and $YbCp_2$ are also given (note the slightly different metal basis sets). The dibromides have been chosen for comparison because of their similar metal charges (see Table V). The relatively large π-bonding contributions (see p_x, p_y, d_{xz}, d_{yz} populations) for the metallocenes represent the most obvious differences between the metallocenes and the dibromides. Larger σ-contributions (see s, p_z, d_{z^2} populations) are observed for the dibromides. Note that the NAO valence populations on the metal generally are very small, consistent with the strongly ionic bonding in the metallocenes.[11]

What are the consequences of the covalent bonding contributions on the degree of bending? As indicated in the introduction, σ-type contributions involving metal d-orbitals contribute significantly to the bending in alkaline earth MX_2 compounds.[6-8] π-Type contributions tend to favor linear arrangements,[9] and these dominate in the metallocenes. This explains why the bending in the metallocenes is considerably reduced compared, e.g., to the corresponding dimethyl compounds.[9] But why do the heavy group 2 and lanthanide metallocenes still exhibit very shallow bending potentials (compared, e.g., to $MgCp_2$[3d]), and why do $BaCp_2$, $SmCp_2$, and $EuCp_2$ even appear to have slightly bent minima? Ligand–ligand repulsions for bent structures are certainly much smaller in these heavy metallocenes than for $MgCp_2$. (As the significant negative charge on the ligands leads to long-range

(34) (a) Kasparov, V. V.; Ezkov, Y. S.; Rambidi, N. G. *Zh. Strukt. Khim.* **1980**, *21*, 41. (b) Kasparov, V. V.; Ezkov, Y. S.; Rambidi, N. G. *Zh. Strukt. Khim.* **1979**, *20*, 260. (c) Lesiecki, M. L.; Nibler, J. W. *J. Chem. Phys.* **1976**, *64*, 871.

(35) Hehre, W. J.; Radom, L.; Schleyer, P. v. R.; Pople, J. A. *Ab Initio Molecular Orbital Theory*, Wiley: New York, 1986.

Table VI. Canonical Molecular Orbital Energies[a] of MCp_2 (M = Ca, Sr, Ba, Sm, Eu, or Yb) at Optimized D_{5d} Structure[b]

(a) M = Ca, Sr, or Ba, Including Metal Subvalence Shell

symm[c]	Ca	character	Sr	character	Ba	character
$3e_{1u}$	−8.22	$L\pi$ + Ca $4p_{x,y}$	−7.92	$L\pi$ + Sr $5p_{x,y}$	−7.59	$L\pi$ + Ba $6p_{x,y}$
$3e_{1g}$	−8.46	$L\pi$ + Ca $3d_{xz,yz}$	−8.33	$L\pi$ + Sr $4d_{xz,yz}$	−8.16	$L\pi$ + Ba $5d_{xz,yz}$
$3a_{2u}$	−13.74	$L\pi$ + Ca $4p_z$	−13.42	$L\pi$ + Sr $5p_z$	−12.95	$L\pi$ + Ba $6p_z$
$2e_{2g}$	−14.04	C–H	−13.88	C–H	−13.71	C–H
$2e_{2u}$	−14.04	C–H	−13.88	C–H	−13.71	C–H
$3a_{1g}$	−14.34	$L\pi$ + Ca 4s	−14.07	$L\pi$ + Sr 5s	−13.77	$L\pi$ + Ba 6s
$2e_{1g}$	−14.83	C–H	−14.67	C–H	−14.48	C–H
$2e_{1u}$	−14.83	C–H	−14.67	C–H	−14.48	C–H
$2a_{2u}$	−19.21	C–C	−19.08	C–C	−18.88	C–C
$2a_{1g}$	−19.24	C–C	−19.08	C–C	−18.88	C–C
$1e_{2u}$	−20.03	C–C	−19.89	C–C	−19.73	C–C
$1e_{2g}$	−20.03	C–C	−19.89	C–C	−19.73	C–C
$1e_{1g}$	−26.18	C–C	−25.96	C–C	−25.82	C–C
$1e_{1u}$	−26.20	C–C	−26.01	C–C	−25.91	C–C + Ba $5p_{x,y}$
$1a_{2u}$	−31.81	C–C	−32.16	C–C + Sr $4p_z$	−31.76	C–C + Ba $5p_z$
$1a_{1g}$	−32.11	C–C	−31.89	C–C	−31.67	C–C
	−35.81	Ca $3p_{x,y}$	−29.17	Sr $4p_{x,y}$	−23.78	Ba $5p_{x,y}$
	−36.00	Ca $3p_z$	−28.71	Sr $4p_z$	−23.65	Ba $5p_z$
	−60.76	Ca 3s	−52.27	Sr 4s	−43.05	Ba 5s

(b) M = Sm, Eu, or Yb, Only Highest Valence MOs

symm	Sm	Eu	Yb	character
$3e_{1u}$	−7.78	−7.81	−8.00	$L\pi$ + M $6p_{x,y}$
$3e_{1g}$	−8.27	−8.27	−8.35	$L\pi$ + M $5d_{xz,yz}$
$3a_{2u}$	−13.22	−13.28	−13.50	$L\pi$ + M $6p_z$
$2e_{2g}$	−13.82	−13.85	−13.93	C–H
$2e_{2u}$	−13.82	−13.85	−13.93	C–H
$2a_{1g}$	−13.99	−14.01	−14.23	$L\pi$ + M 6s

[a] Energies in eV. [b] Hartree–Fock results without f-functions on M and without polarization functions on C and H. [c] The numbering of orbital symmetries follows ref 3d and includes only orbitals mainly concentrated on the ligands. Note, that the ordering of MOs does not always follow the orbital energies.

electrostatic repulsions, typical van der Waals radii for neutral systems may not be very useful for a discussion of such ligand–ligand interactions). However, a nonlinear minimum requires some force to compensate for these repulsions. As discussed above, any stabilization of bent metallocene structures by covalent (σ-) bonding contributions must be small. The polarization of the metal subvalence shell[6,8] is an important factor contributing to the bent structures of some alkaline earth dihalides[8] and dihydrides.[6] With larger metal cations, increasing core polarizability and decreasing ligand–ligand repulsions may contribute to less rigidly linear or even slightly bent structures, in agreement with the observed trends in the bending potentials (cf., e.g., Hartree–Fock results in Table IV) and with the very regular trends of Cp*–M–Cp* angles for the solid-state structures of MCp^*_2 (α = 130.9°, 140.1°, 140.3°, 145°, 147.7° for M = Ba, Sm, Eu, Yb, and Ca, respectively).[4] The covalent bonding contributions for $MgCp_2$ are larger than those for the heavier species, and they mainly involve metal $3p_\pi$-orbitals[3,32] instead of the d_π-orbitals which dominate for the heavier metals. The overlap between the metal p_π-orbitals and the corresponding ligand π-combinations will decrease more sharply upon bending than with d_π-orbitals. This provides an additional reason for the greater rigidity of $MgCp_2$.

E. Canonical MOs and Ionization Potentials. As indicated by the assignment of the canonical valence MOs (see Table VI), the π-type contributions to the metal NAO populations (p_x, p_y, d_{xz}, and d_{yz}) of the metallocenes (cf. Table V) match the symmetries of the highest occupied canonical MOs, $3e_{1u}$(p_x and p_y) and $3e_{1g}$(d_{xz} and d_{yz}). The MO assignments given in Table VI agree with those of previous computational studies of $CaCp_2$,[3d] $YbCp_2$,[11] and $EuCp_2$.[11] The only qualitative difference between our results and those of Blom et al. for calcocene[3d] is the characterization of the $3e_{1u}$ MOs: while Blom et al. described them as pure ligand π-orbitals, our metal p_x and p_y NAO populations (which are about half as large as the d_{xz} and d_{yz} populations, cf. Table V) indicate a small but significant contribution from metal p_π-orbitals. The σ-type contributions are provided by the $3a_{2u}$ and $3a_{1g}$ MOs (with participation of metal p_z and s AOs, respectively). The most obvious change observed along the M = Ca, Yb, Sr, Eu, Sm, and Ba series is the moderate stabilization of the $3e_{1g}$ MOs relative to the other valence orbitals (the difference $\epsilon(3e_{1u})-\epsilon(3e_{1g})$ is 0.24, 0.35, 0.41, 0.46, 0.49, and 0.57 eV along this series). This agrees with the excitation energies of the metal cations[36] and indicates the increasing availability of empty metal d-orbitals to act as acceptors of electron density from the ligands. This in turn may be related to d-orbital contributions to bonding (see preceding section). The HOMO energies for $YbCp_2$ and $EuCp_2$ are ca. 0.9 and 0.8 eV larger than the experimental first ionization potentials of the permethylated species.[11] In view of the very regular trend of the calculated orbital energies for the complete set of the metallocenes, subtraction of ca. 0.8–0.9 eV from the MCp_2 HOMO energy should give reasonable predictions for the first IPs of the other MCp^*_2 species.

Conclusions

Our calculations indicate the equilibrium structures of the heavy group 2 and lanthanide(II) metallocenes either to be linear (M = Ca and Yb) or to be quasilinear (M = Ba, Sm, and Eu). $SrCp_2$ is an intermediate case. Our results do not contradict the experimentally observed bent gas-phase thermal average structures, as the low bending potentials we generally observe may lead to large-amplitude bending motions and considerable shrinkage effects at high temperatures.

The metallocenes are less inclined to be bent than simpler MX_2 compounds (e.g. X = F or CH_3). This is due to the π-character of the covalent bonding contributions in the MCp_2 compounds. Hence, d-orbital participation in bonding does not favor bent MCp_2 geometries to the same extent as for simpler σ-bonded MX_2 systems. The very shallow MCp_2 bending potentials probably are largely determined by cation-polarization effects (which increase with increasing size of the metal cation) and relatively small (compared to, e.g., $MgCp_2$) ligand–ligand repulsions (which de-

(36) Moore, C. E. *Atomic Energy Levels*; Natl. Bur. Stand. Circ. (U.S.) No. 467; National Bureau of Standards: Washington, DC, Vol 1, 1949; Vol 2, 1952.
(37) Langhoff, S. R.; Davidson, E. R. *Int. J. Quant. Chem.* **1974**, *8*, 61.

crease with increasing size of the metal cation).

Williams et al.[4b] argue that the regular trends in the solid-state Cp–M–Cp angles must have intramolecular origins, whereas the strongly irregular trends for the thermal average angles in the gas phase are artifacts due to different temperatures of measurement and the large uncertainties in the bending angles. Our results support this reasoning. Indeed, a regular bending potential trend is found (at least at the HF level of theory, where basis set saturation is comparable for all species). For $CaCp_2$ and $YbCp_2$ (and probably $SrCp_2$) small energy contributions provided by intermolecular interactions are likely to be responsible for the observed bent solid-state structures. $BaCp_2$, $SmCp_2$, and $EuCp_2$ may be slightly bent without intermolecular interactions. However, intermolecular forces certainly contribute to the exact angle observed in the solid state.

All MCp_2 species considered are strongly ionic and structurally nonrigid systems. Discussion of the structures of the growing number of floppy organometallics requires detailed information concerning the experimental or theoretical structure determination, i.e., whether a thermal average or equilibrium structure is involved. This should always be stated explicitly. The energy changes along internal coordinates with shallow potential curves are very useful measures of structural nonrigidity. As this information usually is difficult to obtain experimentally, computational studies will be increasingly helpful.

The NAO populations (cf. Table V) and the valence MO energies of the group 2 and lanthanide(II) metallocenes (cf. Table VI) support the correspondance between the electronic structures of the two sets of molecules. The similarities between group 2 (Ca, Sr, and Ba) and lanthanide(II) (Sm(II), Eu(II), Yb(II)) structural organometallic chemistry have been attributed[1,2] to the ionicity of the compounds and comparable ionic radii of the dications. Additionally, our investigations show that in both sets mainly the $(n-1)$-d-orbitals are employed for donor–acceptor interactions between ligands and dications. Thus, except for the absence of a 4f-shell (with its spectroscopic and synthetic consequences[2]), the Ca, Sr, and Ba organometallics appear to exhibit very similar electronic structures as their Yb(II), Eu(II), and Sm(II) analogues. As lanthanide(II) organometallics (particularly the Sm(II) compounds) are increasingly important for synthetic purposes,[2] the availability of model systems without f-shell may be a useful option.

Acknowledgment. This work was supported by the Deutsche Forschungsgemeinschaft, the Fonds der Chemischen Industrie, the Stiftung Volkswagenwerk and Convex Computer Corporation. M.K. acknowledges a Kekulé grant by the Fonds der Chemischen Industrie. M.D. and H.S. are grateful to Professor H.-J. Werner (Bielefeld) and Professor R. Ahlrichs (Karlsruhe) for providing the MOLPRO and TURBOMOLE program systems.

0002-7863/92/1514-8208$03.00/0